


Article

Optimisation of Glycerol and Itaconic Anhydride Polycondensation

Krzysztof Kolankowski , Magdalena Miętus, Paweł Ruśkowski and Agnieszka Gadomska-Gajadhur * 

Faculty of Chemistry, Warsaw University of Technology, Noakowskiego 3 Street, 00-664 Warsaw, Poland; krzysztof.kolankowski.dokt@pw.edu.pl (K.K.); magdalena.mietus.stud@pw.edu.pl (M.M.); pawel.ruskowski@pw.edu.pl (P.R.)

* Correspondence: agnieszka.gajadhur@pw.edu.pl

Abstract: Glycerol polyesters have recently become objects of interest in tissue engineering. Barely known so far is poly(glycerol itaconate) (PGItc), a biocompatible, biodegradable polyester. Due to the presence of a C=C electron-acceptor moiety, it is possible to post-modify the product by Michael additions to change the properties of PGItc. Thus, using PGItc as one of the elements of cellular scaffold crosslinked in situ for bone tissue regeneration seems to be a very attractive yet unexplored solution. This work aims to optimize the synthesis of PGItc to obtain derivatives with a double bond in the side chain with the highest conversion rates. The experiments were performed with itaconic anhydride and glycerol using mathematical planning of experiments according to the Box-Behnken plan without solvent and catalyst. The input variables of the process were the ratio of the OH/COOH, temperature, and reaction time. The optimised output variables were: the degree of esterification (ED_{titr}), the degree of esterification calculated from the analysis of ^1H NMR spectra (ED_{NMR}), and the degree of itaconic anhydride conversion—calculation based on ^{13}C NMR spectra ($\%X_{^{13}\text{C}}^{\text{NMR}}$). In each of statistical models, the significance of the changed synthesis parameters was determined. Optimal conditions are when OH/COOH ratio is equal to 1.5, temperature is $140\text{ }^\circ\text{C}$ and time of reaction is 5 h. The higher OH/COOH ratio, temperature and longer the experiment time, the higher the value of the degree of esterification and the degree of anhydride conversion.

Keywords: unsaturated glycerol polyesters; poly(glycerol itaconate); design of experiments



Citation: Kolankowski, K.; Miętus, M.; Ruśkowski, P.; Gadomska-Gajadhur, A. Optimisation of Glycerol and Itaconic Anhydride Polycondensation. *Molecules* **2022**, *27*, 4627. <https://doi.org/10.3390/molecules27144627>

Academic Editor: Giuseppe Cirillo

Received: 28 June 2022

Accepted: 18 July 2022

Published: 20 July 2022

Publisher's Note: MDPI stays neutral with regard to jurisdictional claims in published maps and institutional affiliations.



Copyright: © 2022 by the authors. Licensee MDPI, Basel, Switzerland. This article is an open access article distributed under the terms and conditions of the Creative Commons Attribution (CC BY) license (<https://creativecommons.org/licenses/by/4.0/>).

1. Introduction

Glycerol polyesters are a new group of polymers with great potential in medicine. They are biocompatible and biodegradable [1]. Depending on the chain length in dicarboxylic acid, they are characterised by various degradation time in the human body [2]. These polymers can be used short-term (days) or long-term (years) [1,3,4]. Among the polyesters with high biomedical potential can be distinguished, for example poly(glycerol sebacate), poly(glycerol succinate), poly(glycerol fumarate), poly(glycerol maleate), and poly(glycerol itaconate) [5–10].

The substrate for producing these polymers is glycerol, a non-toxic and non-irritating trihydroxy alcohol [11]. Due to the presence of three hydroxyl groups in the structure of glycerol, this compound is hygroscopic and highly soluble in water [12]. Glycerol is the molecular skeleton of fats in the human body. It has antibacterial activity, at which the maximum is observed at $36\text{ }^\circ\text{C}$ (ca human body temperature) [11,12]. It is used in many industries such as food (as a sugar substitute for sweetening beverages), pharmaceutical (drug delivery systems) and cosmetics (as a body care substance) [11,13,14].

The best known and most widely reported in literature is a glycerol-based polyester, poly(glycerol sebacate)—PGS. PGS is a synthetic and biodegradable polymer obtained by the polycondensation of sebacic acid with glycerol (Figure 1) [5,15–22]. PGS exhibits not

only biocompatibility but as well resorbability [23]. Due to its unique properties, PGS is being studied by many researchers for future use in tissue regeneration, both soft (e.g., heart) and hard (e.g., bone) or in the encapsulation of anti-cancer drugs [15,16,19,22,24,25].

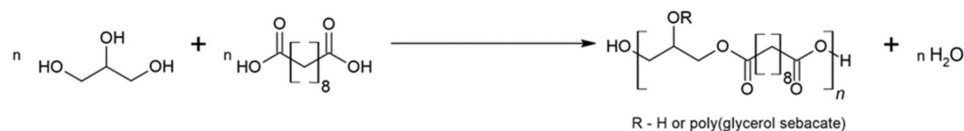


Figure 1. Polycondensation of sebacic acid with glycerol.

The PGS structure consists of hydrophobic (eight methylene groups) and hydrophilic (hydroxyl groups from glycerol) groups [24]. It allows the creation of structures that bind drugs of both hydrophobic and hydrophilic characters [19,24].

A more hydrophilic material is poly(glycerol succinate) (PGSu) [26]. This polymer can be synthesised not only in the reaction between succinic acid and glycerol but also succinic anhydride and glycerol (Figure 2) [26–30]. Like PGS, the synthesis reaction of PGSu occurs without the use of solvent or catalyst [26,31–33]. The functional properties of PGSu are similar to those of PGS. Succinic acid is a natural metabolite in the Krebs cycle; therefore, it is non-toxic to mammalian organisms [34]. The FDA (Food and Drug Administration)-approved succinic acid as a component of medical and pharmaceutical devices [35].



Figure 2. Synthesis of PGSu from succinic anhydride and glycerol.

An attractive alternative to using saturated dicarboxylic acids in synthesising polyesters is the use of dicarboxylic acids containing unsaturated bonds (Figure 3) [36–38]. The use of maleic acid, fumaric acid or itaconic acid may be an example of a substrate for the preparation of innovative polymers [8].

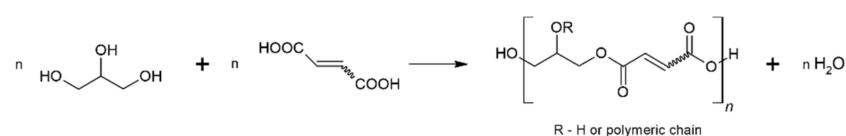


Figure 3. Schematic representation of the synthesis of polyesters with unsaturated bonds.

The double bond is an important element in the poly(glycerol maleate) (PGMal) structure, whose presence enables post-polymerisation reactions [39]. Poly(glycerol fumarate) (PGF) is an isomer of poly(glycerol maleate) (Figure 4) [40]. As in PGMal, a C=C double bond moiety is present in its structure. Poly(glycerol fumarate) can be obtained by reacting glycerol with fumaric acid or fumaric anhydride. Another method to obtain PGF is the reaction of glycerol with maleic anhydride. The Z-mers isomerise to E-mers with increasing temperature and time of the process [41].

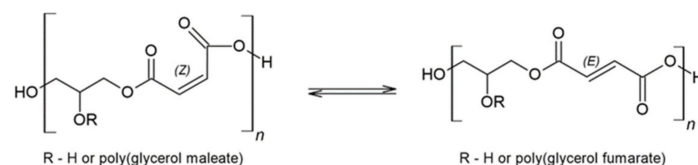


Figure 4. Isomerisation of PGMal and PGF.

Poly(glycerol itaconate) (PGItc) is a curious material because the double bond occurs not in the main chain but in the side chain. It can significantly affect the properties and reactivity of the product compared to PGMal [42,43]. Over the past 30 years, there has been a significant interest in itaconic acid (Figure 5).

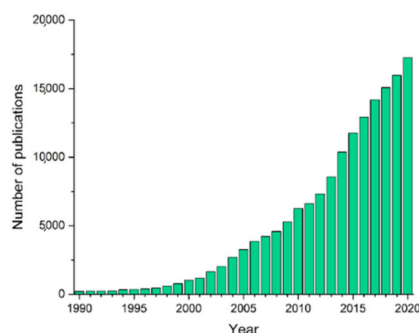


Figure 5. Number of publications with the keyword “itaconic acid” in the years 1990–2020—own elaboration based on data from PubMed.

Itaconic acid can be produced by fermentation by filamentous fungi (most commonly *Aspergillus terreus*) [42,43]. The production volume of acid itself is not significant (due to competitive reactions producing other acids such as maleic or fumaric acid). Still, due to emerging new applications of its derivatives, an increase in demand for itaconic acid is assumed. In 2025, itaconic acid production could be as high as 170 kton/year [42,43].

Itaconic acid is used in medical applications as a hardening agent for contact lenses and as dental cement [44]. Due to its anti-inflammatory and antimicrobial properties, it is believed that itaconic acid can be used to produce various types of drugs [45,46]. In 2020, Wang and his researchers conducted an experiment designed to test the effects of itaconic acid on proteins present in living cells and performing important functions. Itaconic acid caused the modification of a large number of proteins. There were changes in regulatory pathways responsible for the body’s immune response and changes in protein structures responsible for cell death. The polymers based on itaconic acid have a potential for biomedicine applications, e.g., cellular scaffolds. The reaction of itaconic acid or anhydride with glycerol may result in the formation of poly(glycerol itaconate) (PGItc) (Figure 6) [47,48].

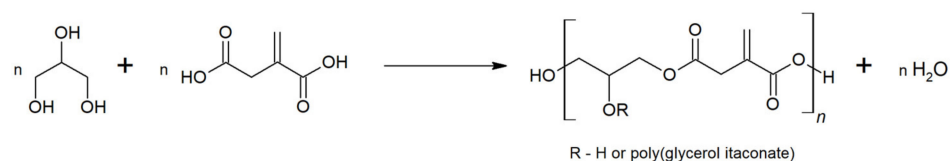


Figure 6. Synthesis of PGItc from glycerol and itaconic acid.

There is a lack of publications directly focused on poly(glycerol itaconate). In contrast, there are many articles describing research on polyitaconates, e.g., based on alkyl groups. Such a compound is, e.g., poly(dodecyl itaconate), which was the subject of a 2015 study led by S. Ramakrishnan [49]. The polymer was obtained by a two-step process. The first step of reaction is conducted with a catalyst (dibutyltin dilaurate, DBTDL) at 150 °C under a nitrogen atmosphere. The oligomerisation reaction involving dibutyl itaconate and 1,12-dodecanediol has taken place. The reaction was then conducted under reduced pressure at 160 °C in the presence of quinol, which was used to prevent the formation of an insoluble polymer. After isolating the product, pure poly(dodecyl itaconate) was obtained.

Itaconate polyesters form rubber-like polymers upon crosslinking. They do not exhibit very high strength, but they can be used in tissue engineering as drug delivery hydrogels [50]. The structure of the growing polymer can be controlled relatively simply by

selecting the molar ratio of glycerol to acid or anhydride. The temperature and time of polycondensation influence the degree of esterification and branching, molecular weight, viscosity, and mechanical properties of PGI_{tc}.

2. Results and Discussion

2.1. FTIR and NMR Analysis

The structure of the obtained polyester was confirmed by the FTIR spectrum (Figure 7).

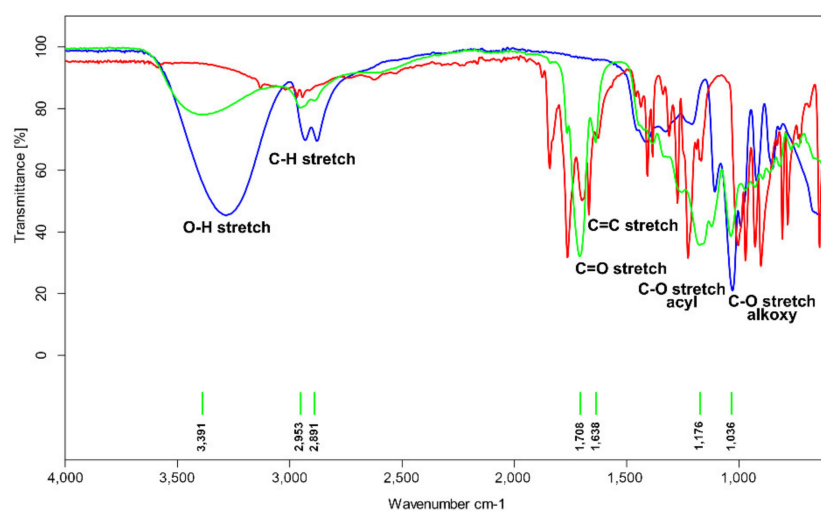


Figure 7. FTIR spectra of poly(glycerol itaconate) (green), itaconic anhydride (red), and glycerol (blue).

The PGI_{tc} spectrum shows a broad band of 3500–3100 cm^{-1} characteristic for hydroxyl group vibrations. The bands 2953 and 2892 cm^{-1} correspond to vibrations of C-H bonds in the main aliphatic chain. The band evidences the presence of an unsaturated C=C bond at 1638 cm^{-1} . The bands at 1709, 1176, and 1036 cm^{-1} are, respectively, the vibration bands of the carbonyl group, acyl, and alkoxy groups.

The interpretation of the ^1H NMR spectra (Figure 8) enabled the confirmation of the product structure and relevant calculations.

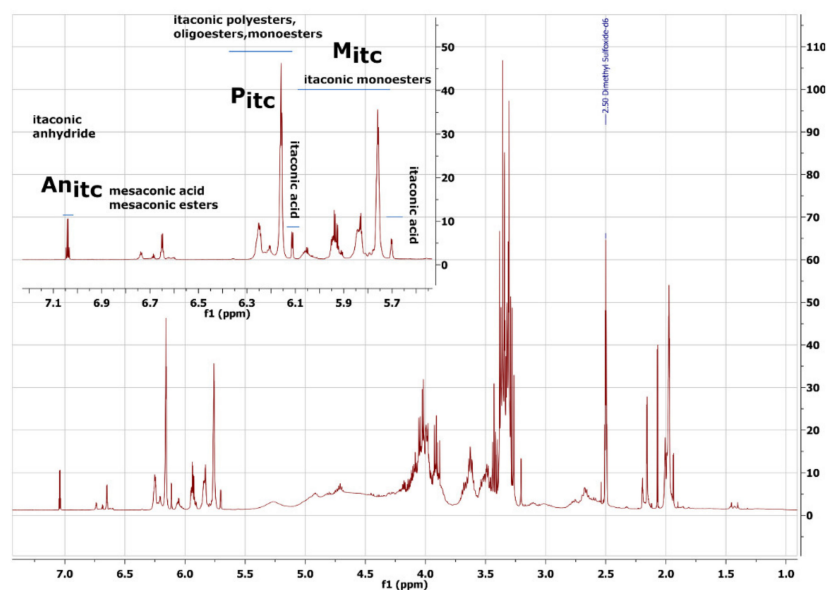


Figure 8. The ^1H NMR spectra of poly(glycerol itaconate).

Glycerol protons are present in the 5.50–4.40 ppm and 4.30–3.20 ppm ranges, and their chemical shift depends on how glycerol is substituted (possible linear, terminal, and dendritic esters). Signals in the range 4.40–4.20 ppm are protons of unreacted glycerol. From 2.3 ppm to 1.9 ppm are CH₂ group protons. The effect of Ordelt saturation occurring (which means the attack of glycerol OH groups on the double bonds) is observed in the range of 3.10–2.53 ppm. The conversion rate of this reaction was calculated and is in the range of 14.2–34.5% (Supplementary Information—Figure S1). We also observe the isomerisation of itaconic fragments to mesaconic fragments. This process occurs with an efficiency of about 1.2–9.8% (Supplementary Information—Figure S1). The higher the process temperature is, the more considerable side reactions become.

Our particular attention was drawn to the signals in the unsaturated bond area. We assigned a defined origin to each of them (Figure 8). The spectra registered for pure reactants were especially useful.

The following formula was used to calculate the esterification degree using NMR spectra.

$$ED_{\text{NMR}} = \left(\frac{\int P_{\text{itc}} + \int M_{\text{itc}}}{\int An_{\text{itc}} + \int M_{\text{itc}} + \int P_{\text{itc}}} \right) \times 100\% \quad (1)$$

where

$\int P_{\text{itc}}$ —The value of the integral of the signal is from the itaconic polyesters, oligoesters, monoesters;

$\int M_{\text{itc}}$ —The value of the integral of the signal is from the itaconic monoesters;

$\int An_{\text{itc}}$ —The value of the integral of the signal is from the itaconic anhydride.

On the ¹³C spectrum (Figure 9), the signals of carbonyl carbons (173–164 ppm), the signals of double bond carbons (136–127 ppm), and the signals of glycerol moiety carbons (76–60 ppm) are observed in sequence.

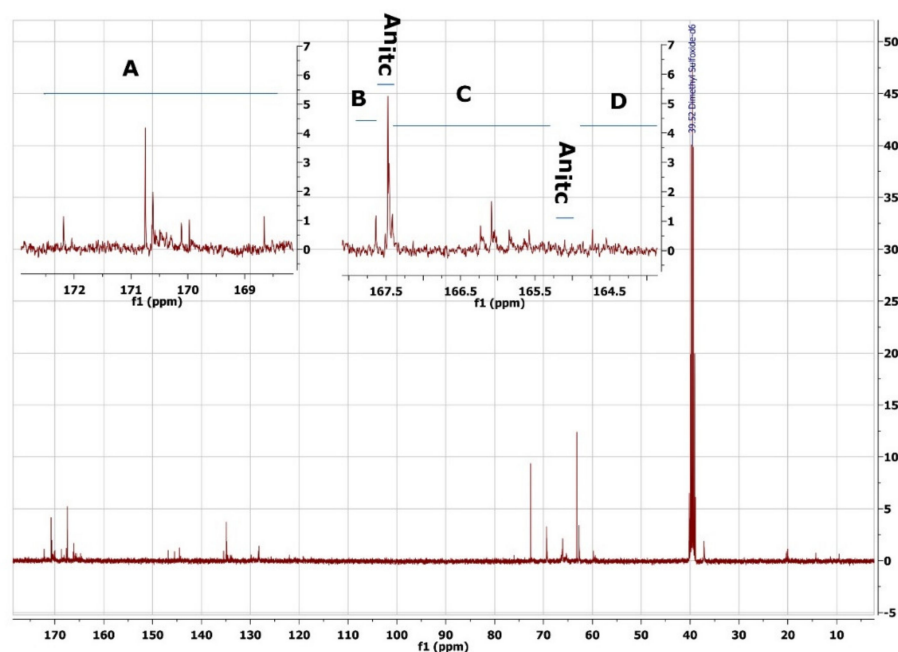


Figure 9. ¹³C NMR spectrum of poly(glycerol itaconate).

The following formula was used to calculate the itaconic anhydride conversion degree,

$$\%X_{13\text{C}}^{\text{NMR}} = \left(\frac{\int A + \int B + \int C + \int D}{\int A + \int B + \int C + \int D + \int An_{\text{itc}}} \right) \times 100\% \quad (2)$$

where

$\int A + \int B + \int C + \int D$ —The value of the integrals of the signals is from the itaconic polyesters, oligoesters, and monoesters;

$\int \text{An}_{\text{itc}}$ —The value of the integral of the signals is from the itaconic anhydride.

2.2. Statistical Analysis

The Box–Behnken plan was used to create mathematical models, as it is the most popular and convenient method of describing the process. The matrix plan consists of 15 experiments, 3 of which are performed under identical conditions to check the repeatability of conditions and the experimenter’s skill.

Such mathematical modelling provides a great deal of valuable information about the object under study and reduces the number of experiments from 27 to 15 (for 3 input variables), which is incredibly precious when scaling up. This saves time and money, which are crucial from the viewpoint of factory economics. The ratio of functional groups, temperature, and time were chosen as input variables because, in our opinion, these variables are easy to control and have the greatest impact on the price of the synthesised product.

The experimentally calculated and model-calculated values of the output variables are summarised in Table 1.

Table 1. Experimental matrix and results (Exp.—experimental, Calc.—calculated).

No.	Coded Variables			ED _{titr} [%]			ED _{NMR} [%]			%X _{13C} ^{NMR} [%]		
	x ₁	x ₂	x ₃	Exp.	Calc.	Rest	Exp.	Calc.	Rest	Exp.	Calc.	Rest
1	−1	−1	0	46.7	49.4	−2.7	68.1	66.7	1.4	57.4	55.6	1.8
2	1	−1	0	51.1	49.4	1.7	70.7	71.2	−0.5	58.5	66.3	−7.8
3	−1	1	0	48.4	49.4	−1.0	65.0	65.3	−0.3	44.2	48.1	−3.9
4	1	1	0	60.9	49.4	11.5	70.4	69.7	0.7	62.2	58.8	3.4
5	−1	0	−1	67.8	63.8	4.0	65.8	66.0	−0.2	52.7	51.8	0.9
6	1	0	−1	19.9	35.0	−15.1	69.7	70.4	−0.7	57.0	62.6	−5.6
7	−1	0	1	44.3	35.0	9.3	64.4	66.0	−1.6	45.4	51.9	−6.5
8	1	0	1	54.0	63.8	−9.8	70.2	70.4	−0.2	64.7	62.6	2.1
9	0	−1	−1	50.1	49.4	0.7	68.0	69.0	−1.0	60.3	61.0	−0.7
10	0	1	−1	48.9	49.4	−0.5	66.5	67.5	−1.0	51.0	53.5	−2.5
11	0	−1	1	43.5	49.4	−5.9	69.7	69.0	0.7	74.0	61.0	13.0
12	0	1	1	60.0	49.4	10.6	68.7	67.5	1.2	62.6	53.5	9.1
13	0	0	0	48.7	49.4	−0.7	68.5	68.2	0.3	57.3	57.2	0.1
14	0	0	0	47.9	49.4	−1.5	68.9	68.2	0.7	54.7	57.2	−2.5
15	0	0	0	48.5	49.4	−0.9	68.7	68.2	0.5	56.2	57.2	−1.0

Based on the Pareto chart analysis (Figure S2), we determined which coefficients of the regression equation are significant. We concluded that only the product of the input variables x_1 and x_3 ($t_{\text{calculated}} = 3.27$) is significant ($t_{\text{calculated}} > t_{\text{critical}}$). It was found that among the input variables, the linear relationship x_1x_3 has the greatest effect on y_1 , so the value of the variable x_2 was set as a constant equal 1).

The equation that describes the degree of esterification defined by titrations methods (y_1) is:

$$y_1 = 49.2 + 14.4 \times x_1 \times x_3 \quad (3)$$

The response surface is the graphic presentation of the calculated model (Figure 10).

Based on the results of the F-test, the adequacy of the model used was determined. The value of F for the equation with one significant variable was 14.94 ($F_{\text{calculated}} < F_{\text{critical}}$), so the applied model can be considered adequate (Tables S1 and S2).

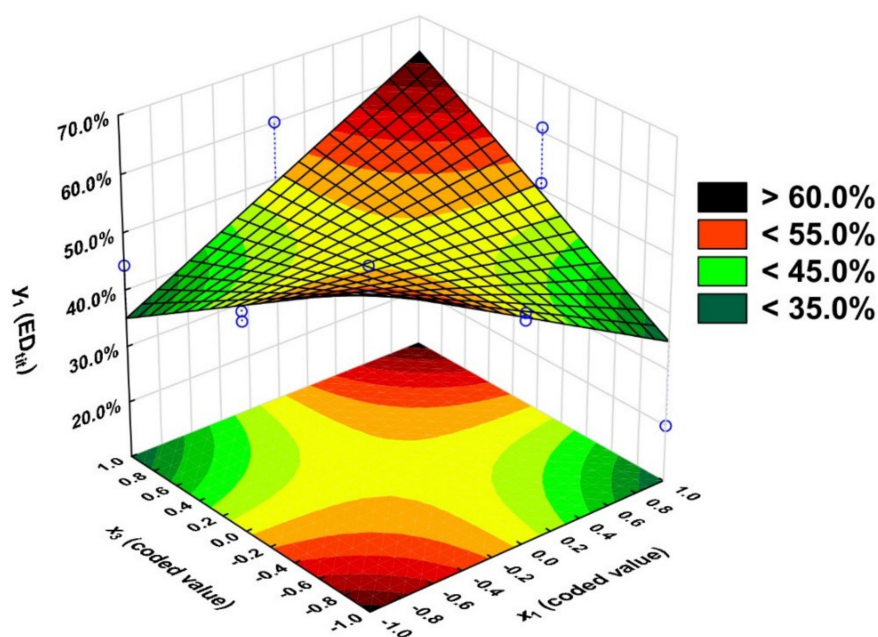


Figure 10. Dependence of esterification degree (ED_{tit}) of PGI_{tc}, on the OH/COOH ratio (x_1) and the time (x_3), $x_2 = 1$.

The coefficient R^2 is 0.53. It means that although only the x_1x_3 relationship is significant; the other input variables and their relationships, although not significant, affect the output variable y_1 .

The esterification values obtained from the titrations were compared with those obtained from the model (Table 1). The experimentally obtained values differ from the approximated values by ± 15.1 percentage points, although for some experiments, the differences are minor (± 0.5 percentage points).

Obtainment of the highest esterification degree is possible when the process is conducted for 5 h with the 1.5 OH/COOH ratio or 3 h and 0.5 OH/COOH ratio— $ED_{tit} > 60.0\%$.

Running the process using a ratio of 1.5 (excess glycerol hydroxyl groups) is associated with a higher ED_{tit} , meaning that linear rather than branched products are more likely to be formed. Running the process for 5 h at a functional group ratio of 0.5 results in an $ED_{tit} < 35.0\%$.

Pareto chart analysis (Figure S3) contributed to the conclusion that the input variable x_1 ($t_{calculated} = 7.56$) has a significant effect on the output variable y_2 ($t_{calculated} > t_{critical}$). The variable x_3 has the least significant effect on the output variable y_2 . Therefore, the time value was set as a constant, $x_3 = 1$. Although the input variable x_2 was insignificant, it was included in the regression equation because the effect score was just below the critical value for the significance level of $p = 0.05$. The addition of the variable x_2 to the regression equation contributed to an increase in the R^2 coefficient from 0.72 to 0.81.

The equation that describes the degree of esterification determined from the analysis of 1H NMR spectra (y_2) takes the following form:

$$y_2 = 68.2 + 2.21 \times x_1 - 0.738 \times x_2 \quad (4)$$

Using the regression equation, the response surface graph was plotted (Figure 11).

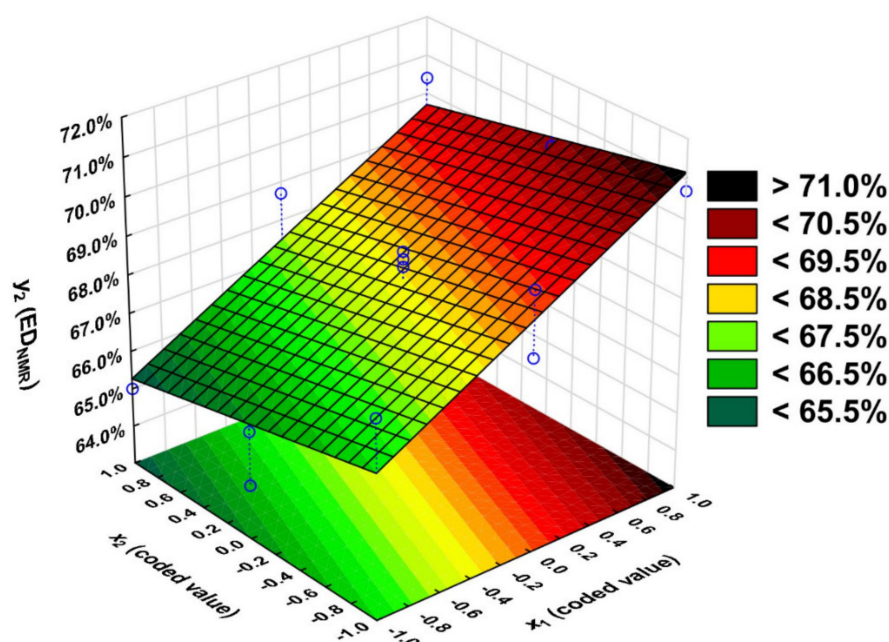


Figure 11. Dependence of esterification degree (ED_{NMR}) of PGItc, on the OH/COOH ratio (x_1) and the temperature (x_2), $x_3 = 1$.

Based on the F-test, we concluded that the calculated value of $F_{calculated}$ for the equation with significant variables is 4.96 and $< F_{critical}$. Thus, the used model is adequate (Tables S3 and S4).

The ED_{NMR} values obtained from the experiments were compared with the values obtained calculated by the model (Table 1). They differ by only ± 1.4 percentage points. The coefficient of determination R^2 is 0.81.

A high ED_{NMR} value ($> 69.5\%$) can be obtained by running the reaction at $140\text{ }^\circ\text{C}$ with an OH/COOH ratio equal to 1.5. By conducting the reaction at $110\text{ }^\circ\text{C}$ with a functional group ratio of 0.5, the ED_{NMR} value is less than 67.5% . The $ED_{NMR} < 65.5\%$ was achieved by conducting the reaction at a functional group ratio of 0.5 at $140\text{ }^\circ\text{C}$.

The Pareto chart analysis determined the significance of the regression equation coefficients (Figure S4). Only the variable x_1 ($t_{critical} = 3.41$) ($t_{calculated} > t_{critical}$) has a statistically significant effect on the degree of itaconic anhydride conversion. The input variable x_2 was also included in the regression equation. However, it was taken into the regression equation due to the substantial increase in the coefficient of R^2 from 0.29 to 0.44.

The equation is of the form:

$$y_3 = 57.1 + 5.35 \times x_1 - 3.76 \times x_2 \quad (5)$$

This equation was used to plot the dependence of the degree of itaconic anhydride conversion (y_3) on the temperature (x_2) and the ratio of functional groups (x_1) for $x_3 = 1$ (Figure 12).

The $F_{calculated}$ value for the equation with significant variables is $6.32 < F_{critical}$, so the model used is adequate (Tables S5 and S6).

The variability of the output variable y_3 is also influenced by other variables and their relationship, although they were insignificant.

The $\%X_{13C}^{NMR}$ values obtained from the model differ from the approximated values by ± 13.0 percentage points, but for some experiments, the differences are ± 0.1 percentage points (Table 1).

The process should be run at the highest functional group ratio at the lowest temperature to obtain the highest $\%X_{13C}^{NMR}$ value. A high $\%X_{13C}^{NMR}$ value cannot be obtained despite high-temperature usage when the functional group ratio is 0.5.

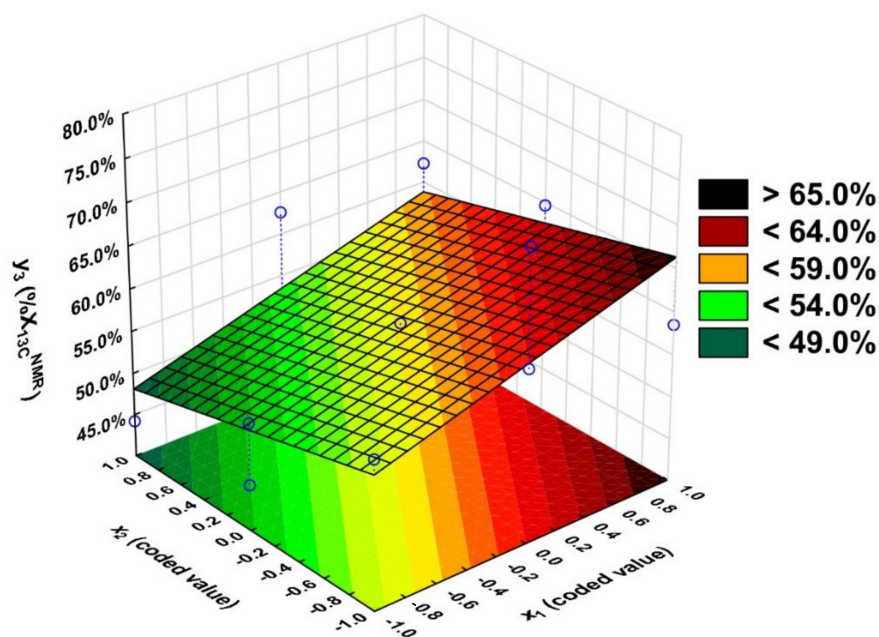


Figure 12. Dependence of itaconic anhydride conversion on the OH/COOH ratio (x_1) and the temperature (x_2), $x_3 = 1$.

2.3. Experiment under Optimal Conditions

Poly(glycerol itaconate), characterised by the highest possible values of the output variables, was obtained by the response utility profile function software (available in Statistica). The utility of the values of output variables was determined (low, medium, and high utility values—Table S7). The highest values obtained in the experimental plan were used as the low utility values of the output variables. We determined that the highest degrees of conversion could be obtained if the synthesis was conducted at a functional group ratio of 1.5 ($x_1 = 1$) at 140 °C ($x_2 = 1$) for 5 h ($x_3 = 1$) (Figure S5).

The experiment was carried out under the assumed conditions, summarising the analysis results in Table 2.

Table 2. Calculated vs. experimental results.

Results	ED _{tit} [%]	ED _{NMR} [%]	%X _{13C} ^{NMR} [%]
Calculated	52.8	69.7	63.0
Experimental	62.3	70.4	62.8

The calculated value of the degree of ED_{tit} esterification is larger than the result calculated from the profile of approximated values by more than ten percentage points. Despite the difference, it can be considered that this value is not significantly different from the expected value. The calculated experimental value of ED_{NMR} differs by 0.7 percentage points from the value calculated using the profile. The experimentally calculated value of the degree of the itaconic anhydride conversion (%X_{13C}^{NMR}) differs from the value calculated using the profile by only 0.2 percentage points.

Received values indicate a good fit of the statistical models to reality.

3. Materials and Methods

3.1. NMR

A nuclear magnetic resonance (NMR) spectroscopy was used. A total of 130–150 mg of product was dissolved in 1 mL of DMSO d-6 (Deutero GmbH, Kastellaun, Germany). The mixture was shaken for 24 h and then transferred to an NMR tube. NMR spectra were

obtained using an Agilent 400 MHz spectrometer. ^{13}C NMR spectra were collected without the nuclear Overhauser effect.

3.2. FTIR

IR spectra were obtained in ATR technics using ALPHA II BRUKER spectrometer. For each sample, 32 scans in the range $400\text{--}4000\text{ cm}^{-1}$ were performed and averaged.

3.3. Acid Number

A total of 0.5–1.5 g of the sample was weighed and dissolved in 25.00 mL of methanol. Then, it was titrated with 1M aqueous NaOH solution until the indicator (thymol blue) turned from yellow to blue. The acid number (AN) was calculated using the following formula:

$$\text{AN} [\text{mgKOH}/\text{g}_{\text{sample}}] = ((V - V_0) \times M_{\text{NaOH}} \times 56.1)/m \quad (6)$$

where

V , the volume of 1 M NaOH solution used to titrate the sample;

V_0 , the volume of 1 M NaOH used for blank titration;

M_{NaOH} , the titer of the solution for the titration (1 M);

56.1, the molar mass of KOH;

m , sample weight.

The final result is the average of three determinations.

3.4. Ester Number

A total of 0.2–0.5 of the sample was weighed and dissolved in 15.00 mL of methanol and 20 mL of 1 M aqueous NaOH solution. The prepared solutions were refluxed for 1 h. Then, the mixture was cooled to room temperature. The excess NaOH was titrated with a 1 M aqueous solution of hydrochloric acid against phenolphthalein until it became discoloured. The ester number (EN) was calculated using the following formula:

$$\text{EN} [\text{mgKOH}/\text{g}_{\text{sample}}] = ((V_0 - V) \times M_{\text{HCl}} \times 56.1)/m - \text{AN} \quad (7)$$

where

V , the volume of 1 M HCl solution used to titrate the sample;

V_0 , the volume of 1 M HCl used for blank titration;

M_{HCl} , the titer of the solution for the titration (1 M);

56.1, the molar mass of KOH;

m , sample weight.

The final result is the average of three determinations.

3.5. Esterification Degree

The ED was calculated according to the following formula:

$$\text{ED} = \text{EN}/(\text{EN} + \text{AN}) \times 100\% \quad (8)$$

where: EN, ester number; AN, acid number.

3.6. Statistical Analysis

Calculations and graphics were made in Statistica 13.1 (StatSoft, Cracow, Poland).

3.7. Synthesis Procedure

PGItc syntheses were carried out in a Mettler Toledo MultiMax parallel reactors system in Hastelloy reactors. Glycerol ($\geq 99\%$, Sigma Aldrich, Burlington, MA, USA), and itaconic anhydride (99%, Ambeed, Arlington Heights, IL, USA) were used without prior preparation (Figure 13). Glycerol (10.62 g, 0.115 mol; 13.53 g, 0.147 mol; 6.45 g 0.070 mol) and itaconic anhydride (19.38 g, 0.173 mol; 16.47 g 0.147 mol; 23.55 g 0.210 mol) were weighed into the

reactor in amounts depending on the molar ratio of the functional groups. Each time, the sum of the reactants was 30.00 g.

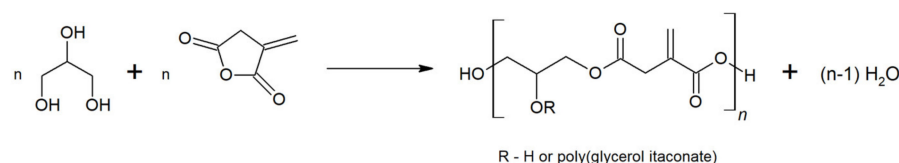


Figure 13. Synthesis of PGIItc from glycerol and itaconic anhydride.

Reactors were equipped with a mechanical stirrer, temperature sensor, and Dean-Stark apparatus. In the first stage, the mixture was heated for over 20 min to temperature x_2 . The temperature was held constant for x_3 hours. After the reaction, the mixture was cooled down to room temperature.

3.8. Optimisation Process

Experiments were planned according to the mathematical methods of planning experiments according to the Box–Behnken plan. The natural values of the variables were coded as -1 , 0 , or $+1$ according to Table 3.

Table 3. Box–Behnken Design—coding values.

Parameter	Natural Variable	Coded Value			Step
		-1	0	$+1$	
x_1	OH/COOH ratio	0.5	1	1.5	0.5
x_2	Temperature [$^{\circ}\text{C}$]	110	125	140	15
x_3	Time [h]	3	4	5	1

4. Conclusions

Three mathematical models were developed to consider the influence of the changed parameters (ratio of functional groups, temperature, and time) on the investigated values (degree of esterification determined by titration methods, degree of esterification received based on ^1H NMR spectra, and degree of itaconic anhydride conversion received based on ^{13}C NMR spectra). All of the obtained models were adequate. The relationship between the ratio of functional groups and the running time of the process has a significant effect on the ED_{titr} value. To obtain the highest ED_{titr} value, the reaction should be carried out for the shortest time (3 h) using the lowest ratio of functional groups (0.5) or carried out for 5 h at a ratio of functional groups of 1.5. Only the ratio of the functional groups of substrates used significantly affects the ED_{NMR} . However, a value close to significant is demonstrated by the temperature variable. The reaction should be carried out at the lowest possible temperature ($110\text{ }^{\circ}\text{C}$) with the highest functional group ratio (1.5) to obtain a high ED_{NMR} value. This conclusion seems illogical and may occur due to the low variability of the ED_{NMR} value. The $\%X_{^{13}\text{C}}^{\text{NMR}}$ value is significantly affected only by the functional group ratio. Since the significance level is a conventional value, the effect of temperature was also considered in determining the regression equation. The regression equation has demonstrated that to obtain a high itaconic anhydride value, the reaction should be carried out at the highest possible ratio of functional groups (1.5), and the process temperature should be $110\text{ }^{\circ}\text{C}$.

The experiment was carried out under optimal conditions, i.e., functional group ratio 1.5, temperature $140\text{ }^{\circ}\text{C}$, and time 5 h, in which $\text{ED}_{\text{titr}} = 62.3\%$, $\text{ED}_{\text{NMR}} = 70.4\%$, and $\%X_{^{13}\text{C}}^{\text{NMR}} = 62.8\%$ were obtained. The values of the obtained variables compared to the predicted values show a good fit of the statistical model to reality.

It could be interesting to extend the experimental area to increase the initial variables' variability and obtain polyester with higher molecular weight. The following research stage will be viscosity and cellular studies of the obtained materials.

Supplementary Materials: The following supporting information can be downloaded at: <https://www.mdpi.com/article/10.3390/molecules27144627/s1>, Figure S1: The ^1H NMR spectra of poly(glycerol itaconate)—side reaction calculations. Figure S2: Pareto chart for the ED_{titr} variable. Figure S3: Pareto chart for the ED_{NMR} variable. Figure S4: Pareto chart for the $\%X_{13\text{C}}^{\text{NMR}}$ variable. Figure S5: Profile of approximated values of input variables and utility. Table S1: Significance test of regression equation coefficients for the ED_{titr} variable. Table S2: Model adequacy test for the ED_{titr} variable. Table S3: Significance test of regression equation coefficients for the ED_{NMR} variable. Table S4: Model adequacy test for the ED_{NMR} variable. Table S5: Significance test of regression equation coefficients for the $\%X_{13\text{C}}^{\text{NMR}}$ variable. Table S6: Model adequacy test for the $\%X_{13\text{C}}^{\text{NMR}}$ variable. Table S7: Values of output variables to generate the response utility profile.

Author Contributions: Conceptualization, K.K. and A.G.-G.; Data curation, K.K. and M.M.; Writing—original draft preparation, K.K., M.M. and A.G.-G.; Supervision and formal analysis, P.R. and A.G.-G.; Methodology, supervision, project administration, writing—review and editing and funding acquisition, A.G.-G.; Validation, P.R., A.G.-G. and K.K. All authors have read and agreed to the published version of the manuscript.

Funding: This scientific research was financed by the National Centre for Research and Development as a research project, “Lider 11” (LIDER/4/0010/L-11/19/NCBR/2020), titled “Porous, biodegradable implants for the regeneration of spongy bone”.

Data Availability Statement: Not applicable.

Conflicts of Interest: The authors declare no conflict of interest.

References

1. Zhang, H.; Grinstaff, M.W. Recent advances in glycerol polymers: Chemistry and biomedical applications. *Macromol Rapid Commun.* **2014**, *35*, 1906–1924. [[CrossRef](#)] [[PubMed](#)]
2. Muthuraj, R.; Valerio, O.; Mekonnen, T.H. Recent developments in short- and medium-chain- length Polyhydroxyalkanoates: Production, properties, and applications. *Int. J. Biol. Macromol.* **2021**, *187*, 422–440. [[CrossRef](#)] [[PubMed](#)]
3. Kim, W.Y.; Muddu, B.N. Eleven-year results of the ABG I hip replacement. *Int. Orthop.* **2006**, *30*, 182–184. [[CrossRef](#)] [[PubMed](#)]
4. Ewend, M.G.; Brem, S.; Gilbert, M.; Goodkin, R.; Penar, P.L.; Varia, M.; Cush, S.; Carey, L.A. Treatment of single brain metastasis with resection, intracavity carmustine polymer wafers, and radiation therapy is safe and provides excellent local control. *Clin. Cancer Res.* **2007**, *13*, 3637–3641. [[CrossRef](#)] [[PubMed](#)]
5. Sundback, C.A.; McFadden, J.; Hart, A.; Kulig, K.M.; Wieland, A.M.; Pereira, M.J.N.; Pomerantseva, I.; Hartnick, C.J.; Masiakos, P.T. Behavior of poly(glycerol sebacate) plugs in chronic tympanic membrane perforations. *J. Biomed. Mater. Res.-Part B Appl. Biomater.* **2012**, *100*, 1943–1954. [[CrossRef](#)] [[PubMed](#)]
6. Wang, Y.; Ameer, G.A.; Sheppard, B.J.; Langer, R. A tough biodegradable elastomer. *Nat. Biotechnol.* **2002**, *20*, 602–606. [[CrossRef](#)]
7. Cai, M.; Liu, H.; Jiang, Y.; Wang, J.; Zhang, S. A high-strength biodegradable thermoset polymer for internal fixation bone screws: Preparation, in vitro and in vivo evaluation. *Colloids Surfaces B Biointerfaces* **2019**, *183*, 110445. [[CrossRef](#)]
8. Hsieh, Y.K.; Hung, P.H.; Huang, C.W.; Chuang, K.C.; Wang, J. Study on the degradation of biodegradable poly (glycerol maleate) (PGM) microbeads. *Polym. Degrad. Stab.* **2020**, *179*, 109223. [[CrossRef](#)]
9. Wang, W.H.; Huang, C.W.; Tsou, E.Y.; Ao-Ieong, W.S.; Hsu, H.C.; Wong, D.S.H.; Wang, J. Characterization of degradation behavior of poly(glycerol maleate) films in various aqueous environments. *Polym. Degrad. Stab.* **2021**, *183*, 1–8. [[CrossRef](#)]
10. Guarneri, A.; Cutifani, V.; Cespugli, M.; Pellis, A.; Vassallo, R.; Asaro, F.; Ebert, C.; Gardossi, L. Functionalization of Enzymatically Synthesized Rigid Poly(itaconate)s via Post-Polymerization Aza-Michael Addition of Primary Amines. *Adv. Synth. Catal.* **2019**, *361*, 2559–2573. [[CrossRef](#)]
11. Pagliaro, M.; Rossi, M. *Glycerol: Properties and Production. The Future of Glycerol*; The Royal Society of Chemistry: London, UK, 2010; pp. 1–28.
12. Fluhr, J.W.; Darlenski, R.; Surber, C. Glycerol and the skin: Holistic approach to its origin and functions. *Br. J. Dermatol.* **2008**, *159*, 23–34. [[CrossRef](#)]
13. Goyal, S.; Hernández, N.B.; Cochran, E.W. An update on the future prospects of glycerol polymers. *Polym. Int.* **2021**, *70*, 911–917. [[CrossRef](#)]
14. García, J.I.; García-Marín, H.; Pires, E. Glycerol based solvents: Synthesis, properties and applications. *Green Chem.* **2014**, *16*, 1007–1033. [[CrossRef](#)]

15. Yeh, Y.C.; Highley, C.B.; Ouyang, L.; Burdick, J.A. 3D printing of photocurable poly(glycerol sebacate) elastomers. *Biofabrication* **2016**, *8*, 045004. [[CrossRef](#)]
16. Chen, Q.Z.; Bismarck, A.; Hansen, U.; Junaid, S.; Tran, M.Q.; Harding, S.E.; Ali, N.N.; Boccaccini, A.R. Characterisation of a soft elastomer poly(glycerol sebacate) designed to match the mechanical properties of myocardial tissue. *Biomaterials* **2008**, *29*, 47–57. [[CrossRef](#)]
17. Gadowska-Gajadhur, A.; Wrzecionek, M.; Matyszczyk, G.; Pietowski, P.; Wieclaw, M.; Ruśkowski, P. Optimization of Poly(glycerol sebacate) Synthesis for Biomedical Purposes with the Design of Experiments. *Org. Process Res. Dev.* **2018**, *22*, 1793–1800. [[CrossRef](#)]
18. Aydin, H.M.; Salimi, K.; Rzaev, Z.M.O.; Pişkin, E. Microwave-assisted rapid synthesis of poly(glycerol-sebacate) elastomers. *Biomater. Sci.* **2013**, *1*, 503–509. [[CrossRef](#)]
19. Louage, B.; Tack, L.; Wang, Y.; De Geest, B.G. Poly(glycerol sebacate) nanoparticles for encapsulation of hydrophobic anti-cancer drugs. *Polym. Chem.* **2017**, *8*, 5033–5038. [[CrossRef](#)]
20. Liang, B.; Shi, Q.; Xu, J.; Chai, Y.M.; Xu, J.G. Poly (Glycerol Sebacate)-Based Bio-Artificial Multiporous Matrix for Bone Regeneration. *Front. Chem.* **2020**, *8*, 1–11. [[CrossRef](#)]
21. Bodakhe, S.; Verma, S.; Garkhal, K.; Samal, S.K.; Sharma, S.S.; Kumar, N. Injectable photocrosslinkable nanocomposite based on poly(glycerol sebacate) fumarate and hydroxyapatite: Development, biocompatibility and bone regeneration in a rat calvarial bone defect model. *Nanomedicine* **2013**, *8*, 1777–1795. [[CrossRef](#)]
22. Li, Y.; Cook, W.D.; Moorhoff, C.; Huang, W.C.; Chen, Q.Z. Synthesis, characterization and properties of biocompatible poly(glycerol sebacate) pre-polymer and gel. *Polym. Int.* **2013**, *62*, 534–547. [[CrossRef](#)]
23. Vogt, L.; Ruther, F.; Salehi, S.; Boccaccini, A.R. Poly(Glycerol Sebacate) in Biomedical Applications—A Review of the Recent Literature. *Adv. Healthc Mater.* **2021**, *10*, 2002026. [[CrossRef](#)]
24. Yang, B.; Lv, W.; Deng, Y. Drug loaded poly(glycerol sebacate) as a local drug delivery system for the treatment of periodontal disease. *RSC Adv.* **2017**, *7*, 37426–37435. [[CrossRef](#)]
25. Rai, R.; Tallawi, M.; Grigore, A.; Boccaccini, A.R. Synthesis, properties and biomedical applications of poly(glycerol sebacate) (PGS): A review. *Prog. Polym. Sci.* **2012**, *37*, 1051–1078. [[CrossRef](#)]
26. Wrzecionek, M.; Howis, J.; Ruskowski, P.; Gadowska-Gajadhur, A. Optimizing the conditions of pgsu synthesis with simplex method. *Chem. Process Eng.-Inz. Chem. Proces.* **2020**, *41*, 119–128. [[CrossRef](#)]
27. Valerio, O.; Horvath, T.; Pond, C.; Misra, M.; Mohanty, A. Improved utilization of crude glycerol from biodiesel industries: Synthesis and characterization of sustainable biobased polyesters. *Ind. Crops Prod.* **2015**, *78*, 141–147. [[CrossRef](#)]
28. Carnahan, M.A.; Grinstaff, M.W. Synthesis of generational polyester dendrimers derived from glycerol and succinic or adipic acid. *Macromolecules.* **2006**, *39*, 609–616. [[CrossRef](#)]
29. Medeiros, E.S.; Offeman, R.D.; Klamczynski, A.P.; Glenn, G.M.; Mattoso, L.H.C.; Orts, W.J. Synthesis, Characterization and Nanocomposite Formation of Poly(glycerol succinate-co-maleate) with Nanocrystalline Cellulose. *J Polym Environ.* **2014**, *22*, 219–226. [[CrossRef](#)]
30. Valerio, O.; Misra, M.; Mohanty, A.K. Sustainable biobased blends of poly(lactic acid) (PLA) and poly(glycerol succinate-co-maleate) (PGSMA) with balanced performance prepared by dynamic vulcanization. *RSC Adv.* **2017**, *7*, 38594–38603. [[CrossRef](#)]
31. Kolbuk, D.; Jeznach, O.; Wrzecionek, M.; Gadowska-Gajadhur, A. Poly(glycerol succinate) as an eco-friendly component of PLLA and PLCL fibres towards medical applications. *Polymers* **2020**, *12*, 1731. [[CrossRef](#)] [[PubMed](#)]
32. Agach, M.; Marinkovic, S.; Estrine, B.; Nardello-Rataj, V. Acyl Poly(Glycerol-Succinic Acid) Oligoesters: Synthesis, Physicochemical and Functional Properties, and Biodegradability. *J. Surfactants Deterg.* **2016**, *19*, 933–941. [[CrossRef](#)]
33. Yin, G.Z.; Yang, X.M.; Zhou, Z.; Li, Q.F. A green pathway to adjust the mechanical properties and degradation rate of PCL by blending bio-sourced poly(glycerol-succinate) oligoesters. *Mater. Chem. Front.* **2018**, *2*, 544–553. [[CrossRef](#)]
34. Chen, S.W.; Xin, Q.; Kong, W.X.; Min, L.; Li, J.F. Anxiolytic-like effect of succinic acid in mice. *Life Sci.* **2003**, *73*, 3257–3264. [[CrossRef](#)] [[PubMed](#)]
35. Zamboulis, A.; Nakiou, E.A.; Christodoulou, E.; Bikiaris, D.N.; Kontonasaki, E.; Liverani, L.; Boccaccini, A.R. Polyglycerol hyperbranched polyesters: Synthesis, properties and pharmaceutical and biomedical applications. *Int. J. Mol. Sci.* **2019**, *20*, 6210. [[CrossRef](#)]
36. Farmer, T.J.; Castle, R.L.; Clark, J.H.; Macquarrie, D.J. Synthesis of unsaturated polyester resins from various bio-derived platform molecules. *Int. J. Mol. Sci.* **2015**, *16*, 14912–14932. [[CrossRef](#)]
37. Tataara, A.M.; Watson, E.; Satish, T.; Scott, D.W.; Kontoyiannis, D.P.; Engel, P.S.; Mikos, A.G. Synthesis and Characterization of Diol-Based Unsaturated Polyesters: Poly(diols fumarate) and Poly(diols fumarate-co-succinate). *Biomacromolecules* **2017**, *18*, 1724–1735. [[CrossRef](#)]
38. Edlund, U.; Albertsson, A.C. Polyesters based on diacid monomers. *Adv. Drug Deliv. Rev.* **2003**, *55*, 585–609. [[CrossRef](#)]
39. Kolankowski, K.; Gadowska-Gajadhur, A.; Wrzecionek, M.; Ruśkowski, P. Mathematically described model of poly(glycerol maleate) cross-linking process using triethylenetetramine addition. *Polym. Adv. Technol.* **2022**, *33*, 1298–1306. [[CrossRef](#)]
40. Feuer, S.S.; Bockstahler, T.E.; Brown, C.A.; Rosenthal, I. Maleic-Fumaric Isomerization in Unsaturated Polyesters. *Ind. Eng. Chem.* **1954**, *46*, 1643–1645. [[CrossRef](#)]
41. Curtis, L.G.; Edwards, D.L.; Simons, R.M.; Trent, P.J.; Von Bramer, P.T. Investigation of maleate-fumarate isomerization in unsaturated polyesters by nuclear magnetic resonance. *Ind. Eng. Chem. Prod. Res. Dev.* **1964**, *3*, 218–221. [[CrossRef](#)]
42. Willke, T.; Vorlop, K.D. Biotechnological production of itaconic acid. *Appl. Microbiol. Biotechnol.* **2001**, *56*, 289–295. [[CrossRef](#)]

43. De Carvalho, J.C.; Magalhães, A.I.; Soccol, C.R. Biobased itaconic acid market and research trends—is it really a promising chemical? *Chim. Oggi-Chem. Today* **2018**, *36*, 56–58.
44. Sriariyanun, M.; Heitz, J.H.; Yasurin, P.; Asavasanti, S.; Tantayotai, P. Itaconic acid: A promising and sustainable platform chemical? *Appl. Sci. Eng. Prog.* **2019**, *12*, 75–82. [[CrossRef](#)]
45. Sano, M.; Tanaka, T.; Ohara, H.; Aso, Y. Itaconic acid derivatives: Structure, function, biosynthesis, and perspectives. *Appl. Microbiol. Biotechnol.* **2020**, *104*, 9041–9051. [[CrossRef](#)]
46. Sano, M.; Yada, R.; Nomura, Y.; Kusakawa, T.; Ando, H.; Matsumoto, K.; Wada, K.; Tanaka, T.; Ohara, H.; Aso, Y. Microbial screening based on the mizoroki–heck reaction permits exploration of hydroxyhexylitaconic-acid-producing fungi in soils. *Microorganisms* **2020**, *8*, 648. [[CrossRef](#)]
47. Qin, W.; Qin, K.; Zhang, Y.; Jia, W.; Chen, Y.; Cheng, B.; Peng, L.; Chen, N.; Liu, Y.; Zhou, W.; et al. S-glycosylation-based cysteine profiling reveals regulation of glycolysis by itaconate. *Nat. Chem. Biol.* **2019**, *15*, 983–991. [[CrossRef](#)]
48. Qin, W.; Zhang, Y.; Tang, H.; Liu, D.; Chen, Y.; Liu, Y.; Wang, C. Chemoproteomic Profiling of Itaconation by Bioorthogonal Probes in Inflammatory Macrophages. *J. Am. Chem. Soc.* **2020**, *142*, 10894–10898. [[CrossRef](#)]
49. Chanda, S.; Ramakrishnan, S. Poly(alkylene itaconate)s—An interesting class of polyesters with periodically located exo-chain double bonds susceptible to Michael addition. *Polym. Chem.* **2015**, *6*, 2108–2114. [[CrossRef](#)]
50. Farmer, T.J.; Macquarrie, D.J.; Comerford, J.W.; Pellis, A.; Clark, J.H. Insights into post-polymerisation modification of bio-based unsaturated itaconate and fumarate polyesters via aza-michael addition: Understanding the effects of C=C isomerisation. *J. Polym. Sci. Part A Polym. Chem.* **2018**, *56*, 1935–1945. [[CrossRef](#)]